Intracerebroventricularly delivered VEGF promotes contralesional corticorubral plasticity after focal cerebral ischemia via mechanisms involving anti-inflammatory actions

Josephine Herz [a], Raluca Reitmeir [a], Sabine I. Hagen [a], Barbara S. Reinboth [a], Zeyun Guo [a], Anil Zechariah [a], Ayman ElAli [a], Thorsten R. Doeppner [a], Marco Bacigaluppi [b], Stefano Pluchino [b], Ülkan Kilic [c], Ertugrul Kilic [d], Dirk M. Hermann [a,*]

[a] Department of Neurology, University Hospital, Essen, Germany
[b] Neuroimmunology Unit and Institute of Experimental Neurology, San Raffaele Scientific Institute, Milan, Italy
[c] Department of Medical Biology, Bezmialem Vakif University, Istanbul, Turkey
[d] Department of Physiology, Yeditepe University, Istanbul, Turkey

ARTICLE INFO

ABSTRACT

Vascular endothelial growth factor (VEGF) has potent angiogenic and neuroprotective effects in the ischemic brain. Its effect on axonal plasticity and neurological recovery in the post-acute stroke phase was unknown. Using behavioral tests combined with anterograde tract tracing studies and with immunohistochemical and molecular biological experiments, we examined effects of a delayed i.c.v. delivery of recombinant human VEGF$_{165}$, starting 3 days after stroke, on functional neurological recovery, corticorubral plasticity and inflammatory brain responses in mice submitted to 30 min of middle cerebral artery occlusion. We herein show that the slowly progressive functional improvements of motor grip strength and coordination, which are induced by VEGF, are accompanied by enhanced sprouting of contralesional corticorubral fibres that branched off the pyramidal tract in order to cross the midline and innervate the ipsilesional parvocellular red nucleus. Infiltrates of CD45+ leukocytes were noticed in the ischemic striatum of vehicle-treated mice that closely corresponded to areas exhibiting Iba-1+ activated microglia. VEGF attenuated the CD45+ leukocyte infiltrates at 14 but not 30 days post ischemia and diminished the microglial activation. Notably, the VEGF-induced anti-inflammatory effect of VEGF was associated with a downregulation of a broad set of inflammatory cytokines and chemokines in both brain hemispheres. These data suggest a link between VEGF's immunosuppressive and plasticity-promoting actions that may be important for successful brain remodeling. Accordingly, growth factors with anti-inflammatory action may be promising therapeutics in the post-acute stroke phase.

Introduction

Upon ischemic stroke, profound remodeling and plasticity processes are induced in the brain parenchyma, which may therapeutically be modulated (Chopp et al., 2008; Hermann and Zechariah, 2009; Lok et al., 2007). This has invigorated hopes that we may become able to promote recovery in stroke patients by means of pharmacological or cell-based interventions. Promising results from experimental studies have rapidly led to clinical trials (Zhang and Chopp, 2009; Zörner and Schwab, 2010), the results of which are eagerly awaited.

Experimental studies gained valuable insights into brain remodeling processes recently. As such, enhanced axonal sprouting was observed contralateral to the stroke in the pyramidal tract of rats after delivery of neutralizing antibodies directed against the growth inhibitory protein Nogo-A (Papadopoulos et al., 2002; Wiessner et al., 2003). Similarly, contralesional pyramidal tract plasticity has been reported after delivery of recombinant human erythropoietin in mice (Reitmeir et al., 2011a), of neural precursor cells in rats (Andres et al., 2011) or of bone marrow-derived stromal cells in rats (Liu et al., 2011). In rodent studies, contralesional plasticity is closely accompanied by behavioral neurological improvements (Reitmeir et al., 2011a; Wiessner et al., 2003). For this reason, axonal plasticity processes are regarded as attractive target for stroke therapies. Until now, the molecular mechanisms controlling axonal growth in the ischemic brain are poorly understood.

Successful recovery is dependent on several ischemia induced processes including the formation of new blood vessels (Hermann

* Corresponding author at: Department of Neurology, University Hospital Essen, Hufelandstr. 55, D-45122 Essen, Germany. Fax: +49 201 723 5534.
   E-mail address: dirk.hermann@uk-essen.de (D.M. Hermann).
   Available online on ScienceDirect (www.sciencedirect.com).

and Zechariah, 2009; Wang et al., 2005), interactions of these vessels with neurons and glial cells (Chopp et al., 2008; Hermann and Zechariah, 2009), the stabilization of new-formed axons against growth repulsive influences (Buchli and Schwab, 2005) and an intact immune surveillance that allows the removal of cell debris without imposing additional damage to the brain tissue (Ceulemans et al., 2010; Dirnagl et al., 1999). Inflammatory responses are triggered by the stroke itself (Ceulemans et al., 2010; Dirnagl et al., 1999; Jordan et al., 2008; Wang et al., 2007a). Adhesion molecules are activated on cerebrovascular cells upon ischemia which together with an increased chemokine production in the brain parenchyma enable immune cell extravasation. These inflammatory responses may potentiate ischemic damage (Dirnagl et al., 1999; Lakhan et al., 2009). Besides, they might also be necessary for brain plasticity and repair (Kriz and Lalancette-Hebert, 2009; Lalancette-Hebert et al., 2007; Madinier et al., 2009)

Vascular endothelial growth factor (VEGF) is a pleiotropic growth factor which is mainly expressed by astrocytes and microglia together with its receptors VEGFR2 and VEGFR1 that are predominantly found on endothelial cells under physiological conditions. Upon hypoxia and ischemia, VEGF and its receptors are rapidly induced within hours on neurons and glial cells (for review see Hermann and Zechariah, 2009). Due to its angiogenic and neuronal survival-promoting properties, VEGF is a promising molecule that allows us to study neurovascular remodeling processes (Sun et al., 2003; Wang et al., 2005, 2007b; Zhang et al., 2000). Whether and how VEGF influences neuronal plasticity after ischemic stroke was unknown.

In the present study we examined the effects of VEGF on pyramidal tract plasticity and inflammatory brain responses. Therefore we performed anterograde tract tracing experiments in order to evaluate pyramidal tract projections from the motor cortex to the red nucleus both ipsilateral and contralateral to the stroke and combined these studies with molecular biological and immunohistochemical experiments. We demonstrate that VEGF induces contralesional but not ipsilesional corticorubral sprouting that is accompanied by anti-inflammatory responses in both hemispheres.

Materials and methods

Animal groups

Experiments were performed in accordance to National Institutes of Health (NIH) Guidelines for the Care and Use of Laboratory Animals with local government approval (Bezirksregierung Düsseldorf, TSG966/08). Male C57Bl6/j mice (8–10 weeks; 23–25 g) were submitted to 30 min of left-sided middle cerebral artery occlusion (MCAO). At 72 h post-ischemia, miniosmotic pumps were implanted into the left lateral ventricle as described below that were filled with 0.9% NaCl or VEGF (0.02 μg/day). The pumps were left in place up to the time point of histochemical and protein expression analysis at 14 and 30 days post ischemia (dpi, n = 3–6 animals/group) or were removed after 30 days for analysis of axonal plasticity at 52 days post-ischemia (n = 10/group). For RT-PCR analysis an additional set of animals was analyzed at 14 and 30 dpi (n = 4/group). A detailed description of groups and sample sizes is presented in Supplemental Fig. S1. For tract-tracing studies additional sham-operated mice receiving pump implantations (filled with vehicle; n = 4 animals) and mice submitted to 30 min MCAO without pump implantation (n = 4 animals) were also generated.

Induction of focal cerebral ischemia

Animals were anesthetized with 1% isoflurane (30% O_2, remainder N_2O). Rectal temperature was maintained between 36.5 and 37.0 °C using a feedback-controlled heating system. Cerebral blood flow was analyzed by laser Doppler flow (LDF) recordings performed above the core of the middle cerebral artery territory using a flexible probe that was attached to the intact animal skull (ElAli and Hermann, 2010; Kilic et al., 2008). LDF changes were monitored during ischemia up to 30 min after reperfusion onset. LDF recordings did not exhibit any differences between groups. Focal cerebral ischemia was induced using an intraluminal filament technique (ElAli and Hermann, 2010; Kilic et al., 2008). Shortly, a midline neck incision was made, and the left common and external carotid arteries were isolated and ligated. A microvascular clip was temporarily placed on the internal carotid artery. A nylon monofilament coated with silicon resin was introduced through a small incision into the common carotid artery (CCA) and advanced to the carotid bifurcation for MCAO. Thirty minutes later, reperfusion was initiated by monofilament removal. In sham-operated animals, the animals' neck was opened and the CCA was exposed, but left intact, while LDF recordings were performed. After the surgery, wounds were carefully sutured, anesthesia was discontinued and animals were placed back into their cages.

Intraventricular pump implantation

Three days after surgery animals were reanesthetized with 1% isoflurane (30% O_2, remainder N_2O) and the cannulae linked to miniosmotic pumps (Alzet 2004 or 2002; Alzet, Cupertino, CA, U.S.A.) filled with 0.9% NaCl or recombinant human $VEGF_{165}$ (PeproTech Inc, USA; 0.02 μg/day in 0.9% NaCl) were implanted into the left lateral ventricle through a bur hole (Kilic et al., 2010). These pumps were left in place for up to four weeks and then removed.

Functional neurological tests

Neurological recovery was assessed at baseline and on 3, 14 and 42 days after MCAO (Reitmeir et al., 2011b).

Grip strength test

The grip strength test consists of a spring balance coupled with a Newtonmeter (Medio-Line Spring Scale, metric, 300 g, Pesola AG, Switzerland) that is attached to a triangular steel wire, which the animal instinctively grasps. Grip strength was evaluated at the right paretic forepaw.

Rota rod test

The rotarod consists of a rotating drum with a speed accelerating from 6 to 40 rpm (Ugo Basile, model 47600, Comerio, Italy), which allows to assess motor coordination skills. The time at which the animal drops off the drum is evaluated (maximum testing time: 300 s).

Delivery of Cascade blue-labeled dextran amine (CB) and biotinylated dextran amine (BDA)

We administered two different tracers, CB and BDA, in the motor cortex both ipsilateral (CB) and contralateral (BDA) to the stroke as previously described (Reitmeir et al., 2011a). Briefly, cranial bur holes were drilled 0.5 mm rostral and 2.5 mm lateral to bregma, via which deposits of 10% BDA or 10% CB (both 10,000 MW; Invitrogen), diluted in 0.01 M phosphate-buffered saline (PBS) at pH 7.2) were placed into the motor cortex by means of microsyringe injections six weeks after MCAO. Ten days after the tracer injection, mice were transcardially perfused with 0.1 M PBS containing 100 I.U. heparin followed by 4% paraformaldehyde in 0.1 M PBS. Brains were removed and post-fixed over-night in 4% paraformaldehyde in 0.1 M PBS and 5% sucrose and cryoprotected in increasing concentrations of sucrose (5%, 10% and 30%) over 3 days. The tissue was then frozen with isopentane and cut into 20 μm and 40 μm thick coronal cryostat sections.

Histochemistry and immunohistochemistry

Immunohistochemistry for CB and BDA

40 μm thick brain sections from animals fixed with 4% paraformaldehyde by transcardiac perfusion were rinsed three times for 10 min each in 50 mM Tris-buffered saline (pH 8.0; TBS) containing 0.5% Triton X-100 (TBST). For detection of CB, sections were immersed overnight at 4 °C with a polyclonal rabbit anti-Cascade blue antibody (1:100, A-5760; Invitrogen, Germany), followed by incubation for one hour at room temperature with a horseradish peroxidase (HRP)-labeled secondary anti-rabbit antibody (1:1000, Santa Cruz Biotech, USA). For detection of BDA, sections were incubated overnight with avidin–biotin–peroxidase complex (ABC Elite; Vector Labs, USA). Stainings were revealed with DAB. Corticorubral projections were evaluated at the level of the parvocellular red nucleus (bregma −3.0 to −3.5 mm). A 500 μm long intersection line was superimposed on the brain midline. Along that line those fibres crossing into the contralateral hemisphere in direction of the red nucleus were quantified. For each animal, the total number of fibres counted was normalized with the total number of labeled fibres in the CST as previously described (Reitmeir et al., 2011a). For both tracers two consecutive sections were analyzed and mean values were determined.

IgG extravasation studies and immunohistochemistry for leukocyte, microglia and astrocyte markers

20 μm cryostat sections taken from the level of the bregma of mice that were transcardially perfused with 0.9% NaCl were used for immunohistochemistries using published fluorescence and avidin–peroxidase protocols (Bacigaluppi et al., 2009; Kilic et al., 2008; Reitmeir et al., 2011a). The following primary antibodies were used: rabbit anti-Iba1 (1:100; Wako, Germany), rat anti-CD45 (1:20, BD Biosciences), rat anti-GFAP (1:500; Invitrogen, Germany), Germany), biotinylated goat anti-mouse IgG (1:150, Santa Cruz Biotech., USA), and biotinylated goat anti-mouse ICAM-1 (1:50, R&D Systems, USA). As secondary antibodies, FITC-conjugated anti-rat (1:100, Jackson Lab., UK) antibody and streptavidin Alexa Fluor 488 (1:100, Invitrogen, Germany) were used for GFAP and ICAM-1 stainings. In immunofluorescence studies, nuclei were counterlabeled with 4′-6-diamidino-2-phenylindole (DAPI) (Roche, Switzerland). For avidin–peroxidase stainings, endogenous peroxidase was blocked with 0.3% hydrogen peroxide in 70% methanol in TBS. Sections were incubated with biotin-conjugated secondary antibodies, immersed with Vectastain®AB kit (Vector Laboratories, USA) and revealed with diamino benzidine tetrahydrochloride (DAB) (Sigma, USA). Sections were evaluated under a bright light and fluorescence microscope (Axioplan; Zeiss, Germany) connected to a CCD camera (Microfire; AVT Horn, Aalen, Germany).

For all stainings, at least 2 sections for each animal were analyzed, for which mean values were determined. For evaluation of GFAP stainings photographs of ipsilateral hemispheres were taken at 2.5× magnification and the GFAP positive area was measured using Image J software (NIH, USA) after conversion into binary images. Data are expressed as percent values of the ischemic striatum. For analysis of ICAM-1, positively stained vessels were counted at 40× magnification in 19 defined regions of interest (ROI, 250,000 μm² each) covering the ischemic area of the striatum. In order to analyze the inflammatory reaction, DAB-labeled CD45 and Iba-1 stainings were analyzed using a bright light microscope at 2.5× magnification and images digitalized with a CCD camera. We analyzed photographs of 9 regions of interest (ROI, 1.03 mm² each) covering the whole striatum of the ipsilateral hemisphere. Images were converted into gray-scale. The inflammatory area was quantified using Image J software (NIH, USA) by limiting the measure to threshold. The high and low thresholds were assigned by determining the average low and high thresholds for the staining procedure and manually recording the ideal threshold values to distinguish inflammatory cells from normal tissue. Data are again expressed as percent values of striatal area per ROI. IgG extravasation was evaluated on photographs taken at 2.5× magnification that were converted into gray scale. On these photographs, mean optical densities for the whole striatum were measured using Image J software (NIH, USA), from which background densities in corresponding non-ischemic areas were subtracted.

Assessment of brain atrophy

On cryostat sections obtained from the level of the bregma (i.e., mid-striatum) that were stained with Iba-1 antibody the outer borders of brain hemispheres were outlined both ipsilateral and contralateral to the stroke and their surface was analyzed (Bacigaluppi et al., 2009). The edema/atrophy index was determined by dividing the area of the ipsilateral hemisphere by that of the contralateral hemisphere and multiplying the result with 100. As such, percentage values were obtained, where values above 100% indicate brain swelling and values below 100% brain atrophy (Bacigaluppi et al., 2009).

Cytokine expression analysis

For cytokine expression studies, tissue samples were harvested from the striatum of mice sacrificed at 14 and 30 dpi by transcardiac perfusion with 0.9% NaCl (n = 4–5 per group). Tissue samples were homogenized and lysated on ice in NP40 lysis buffer containing phosphatase and protease inhibitor cocktails. Protein content was measured using the Bradford method (Biorad, USA). Protein expression was determined using a Cytokine Array Kit (R&D Systems, USA) according to the manufacturer's protocol. Briefly, a total amount of 120 μg per sample was mixed with biotinylated detection antibodies and then incubated with the cytokine array membrane which contains immobilized capture antibodies for the detection of a broad set of inflammatory cytokines and chemokines. Signals were visualized by streptavidin-HRP and chemiluminiscent detection. For each data spot the mean pixel intensity corrected for the background signal was determined using Image J software (NIH, USA). Data were analyzed with mean values from duplicates and related to the mean of three internal control values on each membrane (see also Supplemental Table 1). For graphical presentation fold change ratios were calculated for VEGF-treated ischemic mice as compared to vehicle treated ischemic mice.

Gene expression analysis by RT-PCR

For gene expression studies, mice sacrificed at 3, 14 and 30 days after stroke by transcardiac perfusion with cold 0.1 M PBS containing 0.01 M EDTA (pH 7.4) were used. Brains were quickly removed and dissected on dry-ice. Blocks of tissue were cut from 2 mm rostral to 2 mm caudal to the bregma. From these blocks, samples were collected from six regions of interest, i.e., the striatum, motor cortex and parietal cortex both ipsilateral and contralateral to the stroke. All samples were processed in RNA-later RNA stabilization reagent (#76104; Qiagen, Hilden, Germany) and stored at −80 °C until RNA extraction. Brain tissue samples were homogenized and total RNA was isolated. One μg of cDNA synthesized from 2 μg of total RNA was used for RT-PCR. For quantification of gene expression TaqMan® Gene Expression Assays were used (Mm00443258_m1 TNFa, Mm00449157_m1 VCAM-1, Mm99999055_m1 CXCR4, Mm01336189_m1 IL-1b, Mm00446190_m1 IL-6, Mm01178820 TGFβ, Mm00440485 iNOS). We used glyceraldehyde-3-phosphate dehydrogenase (GAPDH) as housekeeping gene.

RT-PCR was performed using 7900HT Fast-Real-Time PCR System (Applied Biosystems, Darmstadt, Germany). CT values were normalized for endogenous reference [$\Delta CT = CT$ (target gene) $- CT$ (GAPDH)] and compared with a calibrator using the $\Delta\Delta CT$ formula [$\Delta\Delta CT = \Delta CT$ (sample) $- \Delta CT$ (calibrator)]. As calibrator sample we utilized a brain obtained from an untreated mouse of the same age, sex and strain. Data
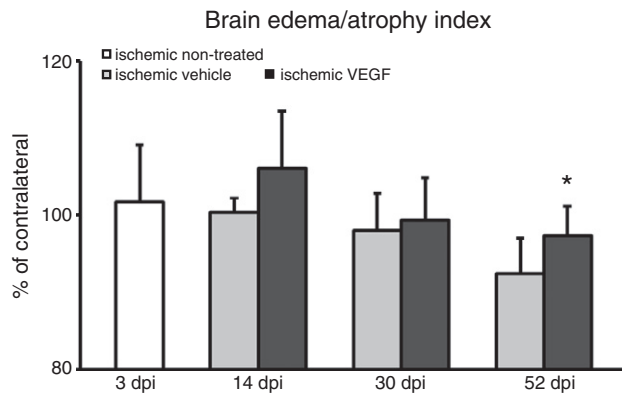
Brain edema/atrophy index

Fig. 1. VEGF reduces brain atrophy. Brain edema/atrophy index at 3, 14, 30 and 52 dpi, expressed as percentage values of contralateral brain tissue. Note that brain atrophy is significantly reduced by VEGF at 52 dpi. Data are means + SD. *p < 0.05 compared with vehicle-treated ischemic mice.

were analyzed using $\log_2$ values of $\Delta\Delta CT$ values (Supplemental Table 2) and fold induction ratios between ischemic VEGF and ischemic vehicle treated animals were calculated for graphical presentation.

Data analysis

Statistical analysis was performed using SPSS 18.0 for Windows (SPSS, Germany). Significance was evaluated by one-way ANOVA followed by LSD post-hoc tests (comparisons with one independent factor and ≥3 groups), by unpaired two-tailed t-tests (comparisons with one independent factor and two groups), or by two way ANOVA followed by unpaired two-tailed t-tests (comparisons with two independent factors). Data are presented as mean and SD values.

Results

VEGF improves functional neurological recovery and prevents secondary neurodegeneration and brain atrophy

As previously shown (Reitmeir et al., 2011b), 30 min of intraluminal MCA occlusion induced mild, but reproducible deficits of motor grip strength in the contralesional right forepaw ($81.0 \pm 12.2\%$ of baseline at 3 dpi) which was accompanied by coordination deficits in Rotarod tests (decrease to $87.0 \pm 18.4\%$ of baseline at 3 dpi). In VEGF-treated animals, motor function progressively improved at 14 and 30 dpi, reaching values significant above control values at 42 dpi (grip strength test: $112.4 \pm 11.1\%$ vs. $87.0 \pm 9.9\%$, Rotarod test: $97.5 \pm 9.7\%$ vs. $83.6 \pm 11.2\%$ of baseline).

Localized brain lesions were obtained in the striatum of ischemic mice that mainly affected the dorsolateral part of the caudate–putamen. In the tissue surrounding the ischemic lesion, secondary neurodegeneration was noticed from 14 dpi to 52 dpi in vehicle-treated ischemic mice which was attenuated by VEGF. As such, VEGF treated mice revealed a significantly reduced brain atrophy at 52 days post-ischemia (Fig. 1).
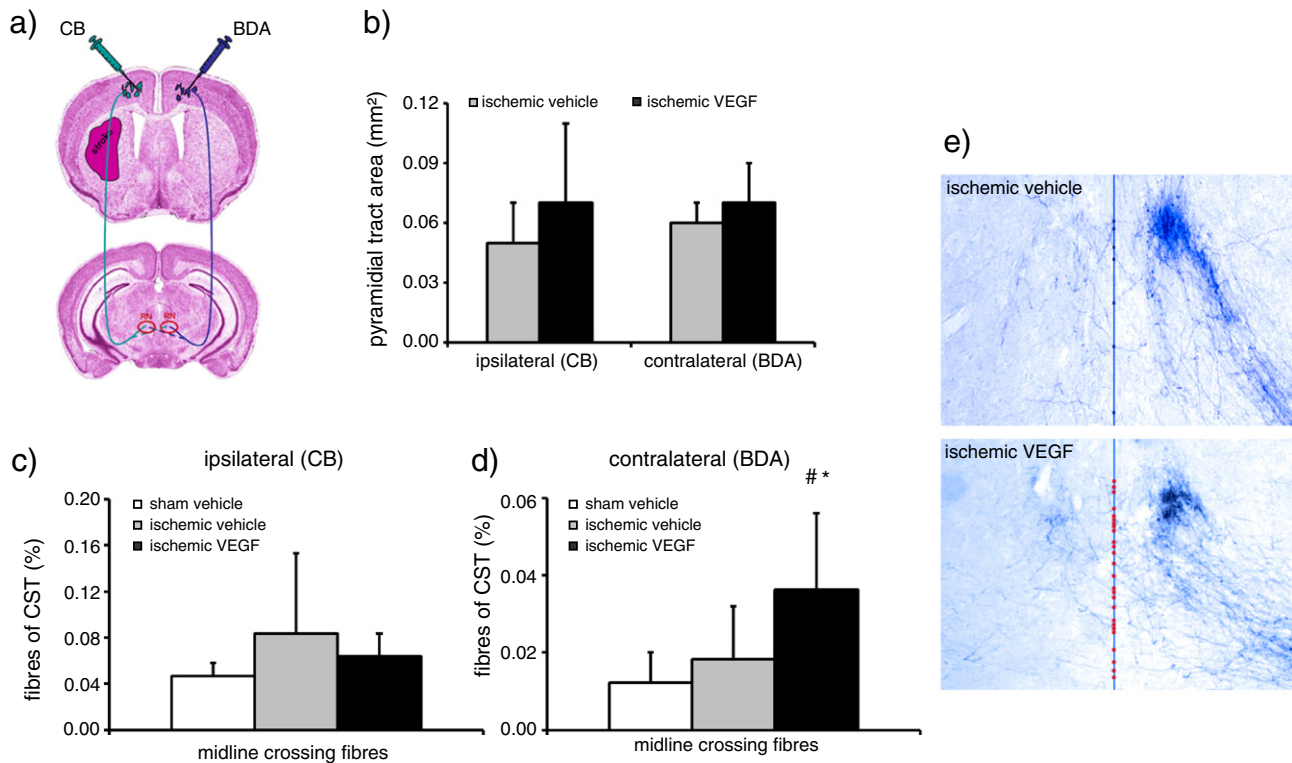

Fig. 2. VEGF promotes contralesional, but not ipsilesional corticorubral plasticity. Tract tracing analysis of corticorubral projections ipsi- and contralateral to the stroke in mice receiving Cascade blue (CB) and biotinylated dextran amine (BDA) injections into the ipsi- and contralateral motor cortex (a). Survival of corticospinal axons is not influenced by VEGF, as demonstrated by analysis of the area covered by the pyramidal tract (b). The percentage of midline crossing fibres after ipsilateral CB injection moderately, but not significantly increases in response to stroke (c). Interestingly, VEGF does not further elevate the percentage of midline-crossing fibres of the ipsilesional pyramidal tract (c), but increases contralateral pyramidal tract sprouting across the midline resulting in fibre outgrowth toward the denervated lesion-sided RN (d). (e) Microphotographs of representative vehicle- and VEGF-treated mice illustrating BDA traced corticorubral fibres intersecting the midline (superimposed in blue) in between both RN. Note that the denervated (left) RN receives more BDA traced fibres after VEGF than after vehicle delivery (midline-intersecting fibres labeled with dots). Data are means + SD. #p < 0.05 compared with vehicle-treated non-ischemic mice. *p < 0.05 compared with vehicle-treated ischemic mice. (For interpretation of the references to color in this figure legend, the reader is referred to the web version of this article.)

VEGF enhances contralesional corticorubral plasticity

To evaluate whether improvements in functional neurological recovery were attributed to changes in axonal plasticity, we analyzed corticorubral plasticity both ipsilateral and contralateral to the stroke by administration of two dextran conjugates, i.e. CB and BDA, that were injected into both motor cortices (Fig. 2a). As described previously (Reitmeir et al., 2011a), injection sites of CB and BDA were obtained that covered the forelimb area and rostral hindlimb area of the primary motor cortex. The number of anterogradely labeled axons in the pyramidal tracts did not differ between vehicle- and VEGF-treated mice, neither ipsilateral nor contralateral to the stroke ($44,453 \pm 19,944$ vs. $44,554 \pm 12,393$ fibres ipsilateral and $88,848 \pm 59,211$ vs. $65,040 \pm 47,039$ fibres contralateral for vehicle and VEGF, respectively). The area covered by the pyramidal tract was similar in both groups (Fig. 2b), indicating that neither ischemia nor VEGF influenced the survival of corticospinal axons. Importantly, VEGF promoted the sprouting of labeled fibres branching off the contralesional (Figs. 2d, e), but not ipsilesional (Fig. 2c) pyramidal tract at the level of the red nucleus. As such, the number of labeled midline-crossing fibres originating from the BDA-labeled contralesional pyramidal tract was significantly increased (Fig. 2d).

VEGF attenuates leukocyte infiltration and microglial activation

Since axonal sprouting might correlate to ischemia-induced astrogliosis and late inflammatory responses in the ischemic brain, we analyzed leukocyte infiltration, microglial activation and reactive astrocytosis in the ischemic striatum by immunohistochemistry for the leukocyte marker CD45, the microglia marker Iba-1 and the astrocyte marker GFAP at 14 and 30 dpi. Infiltrates of CD45+ leukocytes were noticed in the ischemic striatum of vehicle-treated mice at 14 and 30 dpi which closely corresponded to areas exhibiting Iba-1+ immunoreactivity. VEGF reduced infiltration of CD45+ leukocytes into ischemic tissue areas at 14 but not 30 dpi and diminished microglia activation (Figs. 3a, b). In the contralateral hemisphere, no detectable CD45 immunoreactivity and microgliosis were found (not shown). Analysis of the fraction of the GFAP+ area of the striatum did not reveal any difference in astrogliosis between both groups (Fig. 3c).

VEGF does not influence blood–brain barrier integrity and adhesion molecule expression

In acute ischemic stroke, VEGF has previously been shown to increase blood–brain barrier permeability (Wang et al., 2005; Zhang
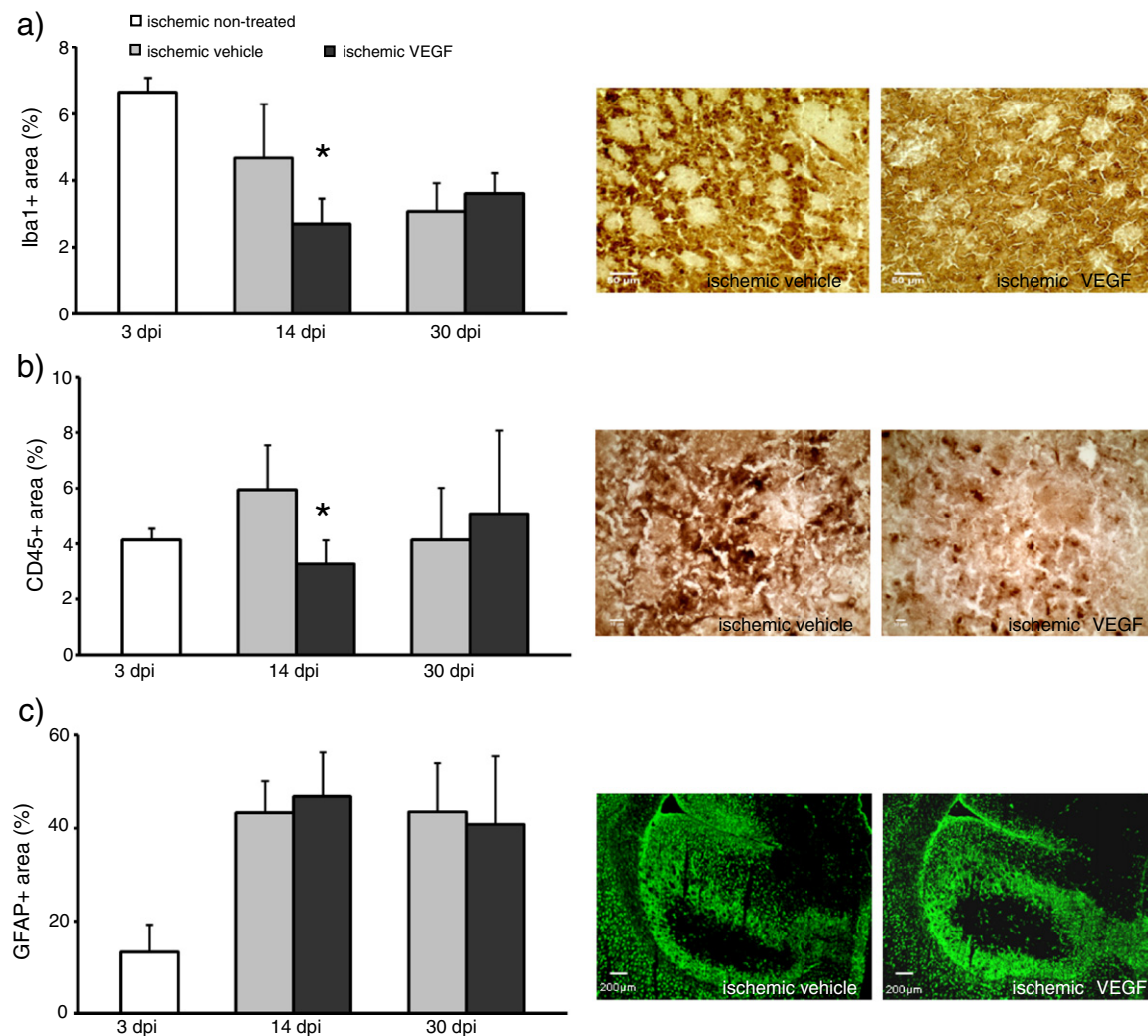

Fig. 3. VEGF reduces leukocyte infiltration and microglia activation at 14 but not 30 days post-ischemia. Quantitative analysis of leukocyte infiltration (a), microglia activation (b) and reactive astrogliosis (c) by means of immunohistochemical stainings for CD45, Iba-1 and GFAP, respectively. Immunohistochemistries were evaluated by determining percent values for immune-positive areas per ROI (for (a) and (b); 9 ROIs; 1.03 mm² each ROI) or of the whole striatum (for (c)). Data are means + SD. *p<0.05 compared with corresponding vehicle. Scale bars, 50 μm (a); 10 μm (b); 200 μm (c).

et al., 2000). To investigate how a chronic delivery of VEGF will influence blood–brain barrier integrity in the post-acute stroke phase, which may facilitate leukocyte brain entry, we subsequently determined IgG extravasation by means of immunohistochemistry. We did not observe any significant changes in IgG extravasation between vehicle-treated and VEGF-treated mice (Fig. 4a). Since IgG extravasation is not necessarily a measure of blood–brain barrier permeability for the transmigration of immune cells, which is actively regulated by adhesion molecules and chemokines, we next checked for the expression of the intracellular cell adhesion molecule-1 (ICAM-1) by immunohistochemistry. Quantification of ICAM-1 positive vessels again did not reveal any differences between vehicle-treated and VEGF-treated mice (Fig. 4b), suggesting that the reduced inflammation we noticed was not induced at the blood–brain interface, but more likely in the brain itself.

VEGF induces a transient suppression of inflammatory cytokines

Since locally delivered VEGF did not modulate vascular properties we next examined how inflammatory mediators in the parenchyma were regulated by VEGF. For this purpose, we performed protein expression analysis for a broad set of inflammatory molecules including cytokines and chemokines. Protein lysates derived from striatal tissues of ipsi- and contralateral hemispheres were individually processed and relative cytokine expression was analyzed by determination of mean pixel intensities corrected for background signals and internal control values (Supplemental Table 1). The mean values of both groups were related to each other resulting in fold change values as presented in Fig. 5. In line with the reduced leukocyte infiltration and microglia activation, we observed a broad suppression of cytokines and chemokines at 14 days post-ischemia. As such, approximately 90% of all proteins were downregulated to values below 80% of control (31/35 of proteins ipsilateral, 32/35 contralateral to the stroke). Besides the downregulation

of pro-inflammatory cytokines, such as IL-6 and IL-12, and hematopoietic cytokines, like GM-CSF, we detected a robust suppression of several chemokines which are known to be crucial for the initiation and propagation of neuroinflammatory processes, supporting leukocyte recruitment to the brain. Among these the most prominent were the CCR2 ligands CCL2 and CCL12 (Fig. 5). Interestingly, the VEGF-mediated immunosuppressive effect disappeared at 30 dpi. We did not detect significant differences between vehicle-treated and VEGF-treated mice at this time point. Notably however, a few cytokines which were strongly down-regulated at 14 dpi, such as IL-6, revealed increased expression levels at 30 dpi after VEGF treatment in the contralateral brain hemi-sphere (Fig. 5).

The anti-inflammatory effect of VEGF is attributed to immunosuppression in the surrounding of the ischemic lesion

Cytokines and chemokines are secreted molecules that are able to move across the brain by passive diffusion over longer distances. To obtain a more detailed idea about the site of VEGF's immunosuppressive actions, we next performed a detailed RT-PCR study, in which we compared how VEGF influenced immune responses in the lesioned striatum, in surrounding cortical tissues and in homologous brain areas contralateral to the stroke (Supplemental Table 2). Notably, profound immunosuppressive effects of VEGF on cytokines such as IL-1β and IL-6 were noticed in the perilesional motor and parietal cortex at 14 dpi, but not in the ischemic striatum. These anti-inflammatory actions disappeared at 30 dpi (Fig. 6). In the brain tissue contralateral to the stroke, no immunosuppressive was found on the mRNA level (Fig. 6). Our data exemplify that mRNA and protein responses do not necessarily go along with each other in the ischemic brain. Evaluations of protein abundance are necessary to evaluate immunomodulatory actions of plasticity-promoting therapies.
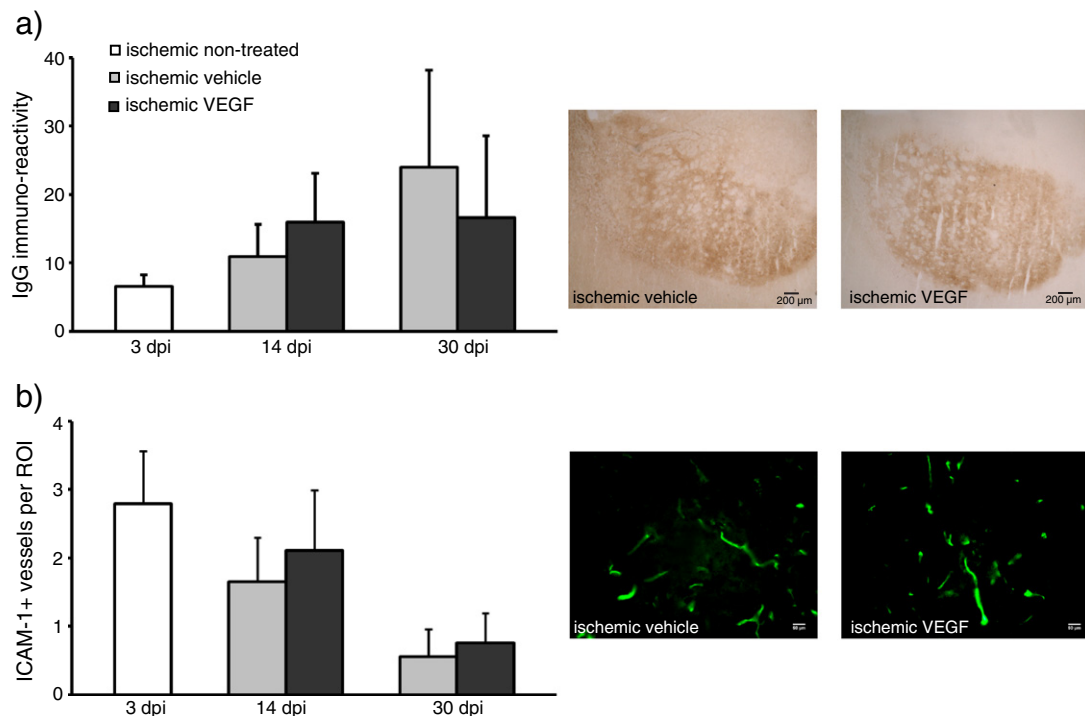

Fig. 4. VEGF does not influence blood–brain barrier integrity and the expression of the adhesion molecule ICAM-1 on brain capillaries. Blood brain barrier permeability for serum IgG (a) and intracellular adhesion molecule-1 (ICAM-1) expression (b) was evaluated by immunohistochemistry. IgG extravasation was densitometrically analyzed and ICAM-1 immunostainings were evaluated by determining the number of ICAM-1+ brain capillaries per region of interest (19 ROIs, 250,000 μm² each). Data are means + SD. Scale bar, 200 μm (a); 50 μm (b).

14 days post ischemia

	CCL1	CCL2	CCL3	CCL4	CCL5	CCL11	CCL12	CCL17	CXCL1	CXCL2	CXCL9	CXCL10	CXCL11	CXCL12	CXCL13
ipsilateral	0.77	0.45	0.44	0.31	0.51	0.63	0.33	0.97	0.66	0.34	0.52	0.56	0.65	0.21	0.55
contralateral	0.74	0.61	0.54	0.38	0.61	0.34	0.36	0.62	0.60	0.55	0.51	0.59	0.69	0.25	0.45

Legend: ≤ 0,40 | > 0,40; ≤ 0,60 | > 0,60; ≤ 0,80 | > 0,80; ≤ 1,00 | > 1,00; ≤ 1,20 | > 1,20; ≤ 1,40 | > 1,4

	M-CSF	G-CSF	GM-CSF	TNF-alpha	IFN-gamma	IL-1 alpha	IL-1 beta	IL-1 ra	IL-2	IL-3	IL-4	IL-6	IL-7	IL-10	IL-13	IL-12 p70	IL-16	IL-17	IL-23	IL-27
ipsilateral	0.46	0.59	0.45	0.88	0.87	0.49	0.53	0.47	0.91	0.69	0.72	0.38	0.61	0.33	0.61	0.29	0.58	0.68	0.71	0.64
contralateral	0.53	0.56	0.41	0.89	0.83	0.52	0.52	0.48	1.06	0.62	0.59	0.32	0.59	0.41	0.52	0.43	0.75	0.53	0.75	0.68

30 days post ischemia

	CCL1	CCL2	CCL3	CCL4	CCL5	CCL11	CCL12	CCL17	CXCL1	CXCL2	CXCL9	CXCL10	CXCL11	CXCL12	CXCL13
ipsilateral	0.86	0.83	0.87	0.86	0.84	1.23	0.86	0.76	0.87	0.95	0.90	0.63	0.77	0.86	0.70
contralateral	1.02	0.92	1.10	1.09	1.06	0.89	0.99	0.88	1.11	1.15	1.18	0.85	0.85	1.32	1.03

Legend: ≤ 0,40 | > 0,40; ≤ 0,60 | > 0,60; ≤ 0,80 | > 0,80; ≤ 1,00 | > 1,00; ≤ 1,20 | > 1,20; ≤ 1,40 | > 1,4

	M-CSF	G-CSF	GM-CSF	TNF-alpha	IFN-gamma	IL-1 alpha	IL-1 beta	IL-1 ra	IL-2	IL-3	IL-4	IL-6	IL-7	IL-10	IL-13	IL-12 p70	IL-16	IL-17	IL-23	IL-27
ipsilateral	0.86	0.84	0.93	0.98	1.01	1.00	0.95	0.77	0.84	0.93	0.85	1.29	0.97	0.89	1.09	0.87	0.92	0.89	1.05	1.14
contralateral	1.32	1.05	1.00	1.06	0.98	1.17	0.98	1.09	0.99	0.98	1.09	1.55	1.05	0.94	1.03	1.31	1.13	0.98	1.18	0.96

Fig. 5. VEGF transiently suppresses inflammatory cytokines and chemokines in both brain hemispheres. Protein abundance analysis of inflammatory cytokines and chemokines by means of a protein array using brain tissue lysates obtained from the ischemic and contralateral striatum at 14 dpi and 30 dpi. Results are presented color-coded as fold change values for VEGF treatment as compared with vehicle. Downregulation may be assumed for values below 0.8 (green and yellow) and upregulation for values above 1.2 (red and brown). Note, that VEGF suppresses protein expression of the majority of inflammatory mediators at 14 dpi, whereas at 30 dpi almost no regulation was detected besides a few cytokines, such as IL-6, that were upregulated in the contralesional hemisphere. For more detailed information on quantitative assessments see also Supplemental Table 1. (For interpretation of the references to color in this figure legend, the reader is referred to the web version of this article.).

Discussion

Using a local low dose VEGF delivery approach which started at the post-acute phase (3 dpi) we herein showed that the functional neurological recovery induced by i.c.v. delivery of recombinant human VEGF is associated with enhanced plasticity of corticorubral fibres branching off the contralesional pyramidal tract in order to innervate the ipsilesional red nucleus. This plasticity promoting effect of VEGF was accompanied by a profound immunosuppressive effect of VEGF in both brain hemispheres.

Seminal studies in rats using models of permanent focal cortical ischemia using neutralizing antibodies directed against the axonal growth inhibitor NogoA revealed that stroke recovery induced by NogoA deactivation was accompanied by enhanced sprouting of contralesional corticorubral, corticobulbar and corticospinal fibres (Markus et al., 2005; Papadopoulos et al., 2002; Seymour et al., 2005; Wiessner et al., 2003). Contralesional pyramidal tract plasticity was found more recently also in mice exposed to transient focal cerebral ischemia that were treated with recombinant human erythropoietin (Reitmeir et al., 2011a) and in rats exposed to permanent focal cerebral ischemia that were treated with bone marrow-derived stromal cells (Liu et al., 2011) or neural precursor cells (Andres et al., 2011). The combined evidence of these studies suggested that the recruitment of intact projections contralateral to the stroke may be more promising for stroke recovery than the repair of previously injured fibre bundles.

Our observation that VEGF promotes contralesional corticorubral sprouting complements an additional study conducted in parallel to the present one, in which we demonstrated that i.c.v. delivery of VEGF also enhances contralesional corticobulbar plasticity at the level of the facial nucleus (Reitmeir et al., 2011b). That plasticity is induced both at the levels of the red and facial nuclei demonstrates that contralesional sprouting was a more general response of the brain to VEGF treatment. In our studies, we observed a profound immunosuppressive effect of VEGF at 14 days after ischemia which was reflected by reduced brain accumulation of inflammatory leukocytes and decreased microglia activation. Although we did not find any changes in blood–brain barrier permeability or ICAM-1 expression on brain capillaries, VEGF induced a broad downregulation of cytokines and chemokines, including GM-CSF, CCL2 and IL-6, which are important for the recruitment and activation of immune cells (Biber et al., 2008; Engelhardt and Ransohoff, 2005).

GM-CSF is a strong inducer of microglia proliferation (Lee et al., 1994), whereas the CCR2 ligand CCL2 acts as chemo-attractant and activator for microglia (Hayashi et al., 1995; Muessel et al., 2002). Recently, a pro-inflammatory role of CCR2 has also been demonstrated in experimental stroke (Dimitrijevic et al., 2007). Thus, the downregulation of GM-CSF and CCL2 well explains the reduced leukocyte infiltration and microglia activation. Immunosuppression is supposed to set the stage for plasticity processes in the ischemic brain. Following delivery of adult neural precursor cells (Bacigaluppi et al., 2009) and delivery of recombinant human erythropoietin (Reitmeir et al.,

14 days post ischemia

ipsilateral		iNOS	TNFa	IL-1b	IL-6	TGFb	CXCR4	VCAM-1
	striatum	1,22	1,09	1,12	1,15	1,03	0,59	1,01
	motor cortex	0,16	0,28	0,19	0,26	0,63	0,16	0,74
	parietal cortex	0,38	0,50	0,14	0,29	0,76	0,55	0,95
contralateral		iNOS	TNFa	IL-1b	IL-6	TGFb	CXCR4	VCAM-1
	striatum	0,88	0,87	1,10	0,73	0,86	0,85	0,85
	motor cortex	1,08	1,43	1,86	1,04	1,15	0,82	0,95
	parietal cortex	0,71	0,58	0,67	0,56	0,71	0,29	0,71

30 days post ischemia

ipsilateral		iNOS	TNFa	IL-1b	IL-6	TGFb	CXCR4	VCAM-1
	striatum	0,72	0,65	0,79	1,17	0,81	0,43	1,22
	motor cortex	0,81	1,45	0,52	1,15	0,99	0,89	1,36
	parietal cortex	0,83	1,87	1,97	1,16	1,21	1,25	1,23
contralateral		iNOS	TNFa	IL-1b	IL-6	TGFb	CXCR4	VCAM-1
	striatum	0,87	0,58	0,72	1,12	0,79	0,65	1,10
	motor cortex	0,55	0,89	0,75	0,97	0,90	0,88	1,19
	parietal cortex	0,72	0,65	0,40	1,10	0,95	0,63	1,24

	≤ 0,40	> 0,40; ≤ 0,60	> 0,60; ≤ 0,80
> 0,80; ≤ 1,00	> 1,00; ≤ 1,20	> 1,20; ≤ 1,40	> 1,4

Fig. 6. VEGF-induced immunosuppression originates in perilesional brain tissue. mRNA expression analysis of cytokines and other inflammatory molecules by means of RT-PCR using brain tissue lysates obtained from the ischemic and contralateral striatum, motor cortex and parietal cortex at 14 dpi and 30 dpi. Results are presented color-coded as fold change values for VEGF treatment as compared with vehicle. Downregulation may be assumed for values below 0.8 (green and yellow) and upregulation for values above 1.2 (red and brown). Note the attenuation of inflammatory gene expression in the perilesional motor cortex and parietal cortex, but not the lesioned striatum at 14 dpi. In the contralesional hemisphere, no clear anti-inflammatory effect of VEGF was observed. For more detailed information on quantitative assessments see also Supplemental Table 2. (For interpretation of the references to color in this figure legend, the reader is referred to the web version of this article.).

2011a), we previously also observed anti-inflammatory effects, which accompanied the neurological recovery. In both studies, only a small set of cytokines and chemokines was examined on the mRNA level. Assessments of protein abundance are crucial for the evaluation of immune responses in the ischemic brain, as we now show. In fact, mRNA and protein responses dissociated from each other in the contralesional hemisphere after VEGF treatment. The dissociation between mRNA and protein responses may partly be explained by the profound suppression of global protein translation after focal cerebral ischemia (Hermann et al., 2001).

The immunosuppressive effect of VEGF disappeared at 30 dpi. At this time, the abundance of some cytokines and chemokines, namely IL-6 and CXCL-12, increased above levels of vehicle-treated mice in the contralesional hemisphere, suggesting a role of these mediators in the promotion of axonal growth. A role of cytokines and chemokines in neuronal plasticity is well established from models of peripheral nerve injury (Boulanger, 2009). In dorsal root ganglion cells, IL-6 and CXCL-12 have specifically been involved in axonal growth (Golz et al., 2006; Opatz et al., 2009). In ischemic stroke, IL-6 is known to have bimodal effects, contributing to the progression of injury in the acute stroke phase but promoting peri-lesional brain remodeling in the post-acute stroke phase (Suzuki et al., 2009). In line with this, we observed a VEGF-induced upregulation of IL-6

which was more pronounced in the contralateral hemisphere, where axonal growth was induced, supporting the idea of IL-6 as a plasticity-promoting cytokine.

Our study does not allow us to establish causal links between immune responses and plasticity processes in the ischemic brain, since we did not modulate immune function. It is conceivable that VEGF also acts directly on axonal growth (Andres et al., 2011), e.g., via its receptor neuropilin-1 (NRP-1), a neuronal surface receptor belonging to the collapsin/semaphorin family of neuritic guidance molecules (Miao et al., 1999; Soker et al., 1998). Our results show that immune responses accompanying brain plasticity are finely tuned in time and space. This observation deserves notion in the development of plasticity-promoting therapies. For the successful translation of plasticity-promoting therapies from rodents to human patients, closer insights into mechanisms controlling these axonal sprouting and brain remodeling processes are urgently required.

This study is not meant to prepare a clinical proof-of-concept study in human patients. From a translational point of view, experiments with other application routes, i.e., systemic delivery, and perhaps also a stroke model that is more closely related to clinical stroke conditions, such as cerebral thromboembolism, would be needed. With respect to its clinical applicability, it should also be kept in mind that VEGF may have deleterious side effects, inducing

vascular permeability, brain hemorrhage and inflammation, when administered at the wrong time point (i.e., in the acute phase, immediately after the stroke) via systemic delivery (Abumiya et al., 2005; Zhang et al., 2000). In view of VEGF's potent actions on neurons and vessels, representing a growth factor that is de novo expressed as part of an endogenous brain response after focal cerebral ischemia (Hermann and Zechariah, 2009), the present study provides a further proof of principle that the promotion of brain plasticity and recovery post stroke is feasible. As such, growth factors might represent promising alternatives to cell-based therapies.

Supplementary materials related to this article can be found online at doi:10.1016/j.nbd.2011.12.026.

Acknowledgments

References

Abumiya, T., Yokota, C., Kuge, Y., Minematsu, K., 2005. Aggravation of hemorrhagic transformation by early intraarterial infusion of low-dose vascular endothelial growth factor after transient focal cerebral ischemia in rats. Brain Res. 1049, 95–103.

Andres, R.H., Horie, N., Slikker, W., Keren-Gill, H., Zhan, K., Sun, G., Manley, N.C., Pereira, M.P., Sheikh, L.S., McMIllan, E.L., Schaar, B.T., Svendsen, C.N., Bliss, T.M., Steinberg, G.K., 2011. Human neural stem cells enhance structural plasticity and axonal transport in the ischaemic brain. Brain 134, 1777–1789.

Bacigaluppi, M., Pluchino, S., Peruzzotti-Jametti, L., Kilic, E., Kilic, U., Salani, G., Brambilla, E., West, M.J., Comi, G., Martino, G., Hermann, D.M., 2009. Delayed post-ischaemic neuroprotection following systemic neural stem cell transplantation involves multiple mechanisms. Brain 132, 2239–2251.

Biber, K., Vinet, J., Boddeke, H.W., 2008. Neuron–microglia signaling: chemokines as versatile messengers. J. Neuroimmunol. 198, 69–74.

Boulanger, L.M., 2009. Immune proteins in brain development and synaptic plasticity. Neuron 64, 93–109.

Buchli, A.D., Schwab, M.E., 2005. Inhibition of Nogo: a key strategy to increase regeneration, plasticity and functional recovery of the lesioned central nervous system. Ann. Med. 37, 556–567.

Ceulemans, A.G., Zgavc, T., Kooijman, R., Hachimi-Idrissi, S., Sarre, S., Michotte, Y., 2010. The dual role of the neuroinflammatory response after ischemic stroke: modulatory effects of hypothermia. J. Neuroinflammation 7, 74.

Chopp, M., Li, Y., Zhang, J., 2008. Plasticity and remodeling of brain. J. Neurol. Sci. 265, 97–101.

Dimitrijevic, O.B., Stamatovic, S.M., Keep, R.F., Andjelkovic, A.V., 2007. Absence of the chemokine receptor CCR2 protects against cerebral ischemia/reperfusion injury in mice. Stroke 38, 1345–1353.

Dirnagl, U., Iadecola, C., Moskowitz, M.A., 1999. Pathobiology of ischaemic stroke: an integrated view. Trends Neurosci. 22, 391–397.

ElAli, A., Hermann, D.M., 2010. Apolipoprotein E controls ATP-binding cassette transporters in the ischemic brain. Sci. Signal. 3, ra72.

Engelhardt, B., Ransohoff, R.M., 2005. The ins and outs of T-lymphocyte trafficking to the CNS: anatomical sites and molecular mechanisms. Trends Immunol. 26, 485–495.

Golz, G., Uhlmann, L., Ludecke, D., Markgraf, N., Nitsch, R., Hendrix, S., 2006. The cytokine/neurotrophin axis in peripheral axon outgrowth. Eur. J. Neurosci. 24, 2721–2730.

Hayashi, M., Luo, Y., Laning, J., Strieter, R.M., Dorf, M.E., 1995. Production and function of monocyte chemoattractant protein-1 and other beta-chemokines in murine glial cells. J. Neuroimmunol. 60, 143–150.

Hermann, D.M., Zechariah, A., 2009. Implications of vascular endothelial growth factor for postischemic neurovascular remodeling. J. Cereb. Blood Flow Metab. 29, 1620–1643.

Hermann, D.M., Kilic, E., Hata, R., Hossmann, K.A., Mies, G., 2001. Relationship between metabolic dysfunctions, gene responses and delayed cell death after mild focal cerebral ischemia in mice. Neuroscience 104, 947–955.

Jordan, J., Segura, T., Brea, D., Galindo, M.F., Castillo, J., 2008. Inflammation as therapeutic objective in stroke. Curr. Pharm. Des. 14, 3549–3564.

Kilic, E., Spudich, A., Kilic, U., Rentsch, K.M., Vig, R., Matter, C.M., Wunderli-Allenspach, H., Fritschy, J.M., Bassetti, C., Hermann, D.M., 2008. ABCC1: a gateway for pharmacological compounds to the ischaemic brain. Brain 131, 2679–2689.

Kilic, E., ElAli, A., Kilic, U., Guo, Z., Ugur, M., Uslu, U., Bassetti, C.L., Schwab, M.E., Hermann, D.M., 2010. Role of Nogo-A in neuronal survival in the reperfused ischemic brain. J. Cereb. Blood Flow Metab. 30, 969–984.

Kriz, J., Lalancette-Hebert, M., 2009. Inflammation, plasticity and real-time imaging after cerebral ischemia. Acta Neuropathol. 117, 497–509.

Lakhan, S.E., Kirchgessner, A., Hofer, M., 2009. Inflammatory mechanisms in ischemic stroke: therapeutic approaches. J. Transl. Med. 7, 97.

Lalancette-Hebert, M., Gowing, G., Simard, A., Weng, Y.C., Kriz, J., 2007. Selective ablation of proliferating microglial cells exacerbates ischemic injury in the brain. J. Neurosci. 27, 2596–2605.

Lee, S.C., Liu, W., Brosnan, C.F., Dickson, D.W., 1994. GM-CSF promotes proliferation of human fetal and adult microglia in primary cultures. Glia 12, 309–318.

Liu, Z., Li, Y., Zhang, R.L., Cui, Y., Chopp, M., 2011. Bone marrow stromal cells promote skilled motor recovery and enhance contralesional axonal connections after ischemic stroke in adult mice. Stroke 42, 740–744.

Lok, J., Gupta, P., Guo, S., Kim, W.J., Whalen, M.J., van Leyen, K., Lo, E.H., 2007. Cell–cell signaling in the neurovascular unit. Neurochem. Res. 32, 2032–2045.

Madinier, A., Bertrand, N., Mossiat, C., Prigent-Tessier, A., Beley, A., Marie, C., Garnier, P., 2009. Microglial involvement in neuroplastic changes following focal brain ischemia in rats. PLoS One 4, e8101.

Markus, T.M., Tsai, S.Y., Bollnow, M.R., Farrer, R.G., O'Brien, T.E., Kindler-Baumann, D.R., Rausch, M., Rudin, M., Wiessner, C., Mir, A.K., Schwab, M.E., Kartje, G.L., 2005. Recovery and brain reorganization after stroke in adult and aged rats. Ann. Neurol. 58, 950–953.

Miao, H.Q., Soker, S., Feiner, L., Alonso, J.L., Raper, J.A., Klagsbrun, M., 1999. Neuropilin-1 mediates collapsin-1/semaphorin III inhibition of endothelial cell motility: functional competition of collapsin-1 and vascular endothelial growth factor-165. J. Cell Biol. 146, 233–242.

Muessel, M.J., Klein, R.M., Wilson, A.M., Berman, N.E., 2002. Ablation of the chemokine monocyte chemoattractant protein-1 delays retrograde neuronal degeneration, attenuates microglial activation, and alters expression of cell death molecules. Brain Res. Mol. Brain Res. 103, 12–27.

Opatz, J., Kury, P., Schiwy, N., Järve, A., Estrada, V., Brazda, N., Bosse, F., Müller, H.W., 2009. SDF-1 stimulates neurite growth on inhibitory CNS myelin. Mol. Cell. Neurosci. 40, 293–300.

Papadopoulos, C.M., Tsai, S.Y., Alsbiei, T., O'Brien, T.E., Schwab, M.E., Kartje, G.L., 2002. Functional recovery and neuroanatomical plasticity following middle cerebral artery occlusion and IN-1 antibody treatment in the adult rat. Ann. Neurol. 51, 433–441.

Reitmeir, R., Kilic, E., Kilic, U., Bacigaluppi, M., ElAli, A., Salani, G., Pluchino, S., Gassmann, M., Hermann, D.M., 2011a. Post-acute delivery of erythropoietin induces stroke recovery by promoting perilesional tissue remodelling and contralesional pyramidal tract plasticity. Brain 134, 84–99.

Reitmeir, R., Kilic, E., Reinboth, B.S., Guo, Z., ElAli, A., Zechariah, A., Kilic, U., Hermann, D.M., 2011b. Vascular endothelial growth factor induces contralesional corticobulbar plasticity and functional neurological recovery in the ischemic brain. Acta Neuropathol. doi:10.1007/s00401-011-0914-z.

Seymour, A.B., Andrews, E.M., Tsai, S.Y., Markus, T.M., Bollnow, M.R., Brennemann, M.R., O'Brien, T.E., Castro, A.J., Schwab, M.E., Kartje, G.L., 2005. Delayed treatment with monoclonal antibody IN-1 1 week after stroke results in recovery of function and corticorubral plasticity in adult rats. J. Cereb. Blood Flow Metab. 25, 1366–1375.

Soker, S., Takashima, S., Miao, H.Q., Neufeld, G., Klagsbrun, M., 1998. Neuropilin-1 is expressed by endothelial and tumor cells as an isoform-specific receptor for vascular endothelial growth factor. Cell 92, 735–745.

Sun, Y., Jin, K., Xie, L., Childs, J., Mao, X.O., Logvinova, A., Greenberg, D.A., 2003. VEGF-induced neuroprotection, neurogenesis, and angiogenesis after focal cerebral ischemia. J. Clin. Invest. 111, 1843–1851.

Suzuki, S., Tanaka, K., Suzuki, N., 2009. Ambivalent aspects of interleukin-6 in cerebral ischemia: inflammatory versus neurotrophic aspects. J. Cereb. Blood Flow Metab. 29, 464–479.

Wang, Y., Kilic, E., Kilic, U., Weber, B., Bassetti, C.L., Marti, H.H., Hermann, D.M., 2005. VEGF overexpression induces post-ischaemic neuroprotection, but facilitates haemodynamic steal phenomena. Brain 128, 52–63.

Wang, Q., Tang, X.N., Yenari, M.A., 2007a. The inflammatory response in stroke. J. Neuroimmunol. 184, 53–68.

Wang, Y., Jin, K., Mao, X.O., Xie, L., Banwait, S., Marti, H.H., Greenberg, D.A., 2007b. VEGF-overexpressing transgenic mice show enhanced post-ischemic neurogenesis and neuromigration. J. Neurosci. Res. 85, 740–747.

Wiessner, C., Bareyre, F.M., Allegrini, P.R., Mir, A.K., Frentzel, S., Zurini, M., Schnell, L., Oertle, T., Schwab, M.E., 2003. Anti-Nogo-A antibody infusion 24 hours after experimental stroke improved behavioral outcome and corticospinal plasticity in normotensive and spontaneously hypertensive rats. J. Cereb. Blood Flow Metab. 23, 154–165.

Zhang, Z.G., Chopp, M., 2009. Neurorestorative therapies for stroke: underlying mechanisms and translation to the clinic. Lancet Neurol. 8, 491–500.

Zhang, Z.G., Zhang, L., Jiang, Q., Zhang, R., Davies, K., Powers, C., Bruggen, N., Chopp, M., 2000. VEGF enhances angiogenesis and promotes blood–brain barrier leakage in the ischemic brain. J. Clin. Invest. 106, 829–838.

Zörner, B., Schwab, M.E., 2010. Anti-Nogo on the go: from animal models to a clinical trial. Ann. N. Y. Acad. Sci. 1198, E22–E34.